Forward Modelling of the Earth's Topographic Gravitational Potential Using Confocal Ellipsoidal Surfaces up to degree and order 3660

Oleh Abrykosov, Christoph Förste, E. Sinem Ince and Frank Flechtner
Section 1.2: Global Geomonitoing and Gravity Field
Department1: Geodesy

Gravity Forward Modelling

- Computation of global gravitational field model using source mass distribution (not actual gravity measurements)
- Geometry of the Earth's body and suitable mass-density values are used to represent the gravitational field based on Newton's law of gravitation
- Can be realised in spatial or spectral domain, both require global coverage of the mass-density information

- **General use:** Modelling Earth's or other planets' gravity field potential
  - topographic potential model → from a high resolution topography model (DEM)

Our purpose

The gravity forward modelling has become widely used for or due to the following reasons:

1. To construct detailed gravity or gravity field functional maps, in other words, to **retrieve high frequency components of the gravitational field** (i.e. to reduce the omission error)
2. To interpolate or **predict gravity values in the regions that have limited or no gravity measurements,**
3. To reduce gravity measurements for the topographical effect, i.e.
   a) to develop Bouguer gravity anomaly maps (or models)
   b) to reduce the data for high frequency components before gridding

Content

- Development of GFZ’s topographic gravity field model (ROLI_SphN_3660) based on multi layer approach in spectral domain
- Comparison with other similar models of its kind
- Development of blended model using EIGEN-6C4 and ROLI
  - development of new generation high resolution static global gravity field models, EIGEN-x
- Evaluation of blended model using external dataset

ROLI Topographic Gravity Field Model (1)

- ROLI (Rock Ocean Lake Ice) model is developed based on multi layer approach and it represents the topographic gravity field model up to d/o 3660
- Newton's integral is expressed for the masses located between the bounding ellipsoid (external to all source masses) and the lower most boundary ellipsoid

$$V(b,\vartheta_b,\lambda_b) = G\iiint \frac{\rho(u,\vartheta,\lambda)}{\ell(b,\vartheta_b,\lambda_b,u,\vartheta,\lambda)}\,dv$$

$$dv = \left(u^2 + E^2\cos^2\vartheta\right)\sin\vartheta\, d\vartheta\, d\lambda\, du$$

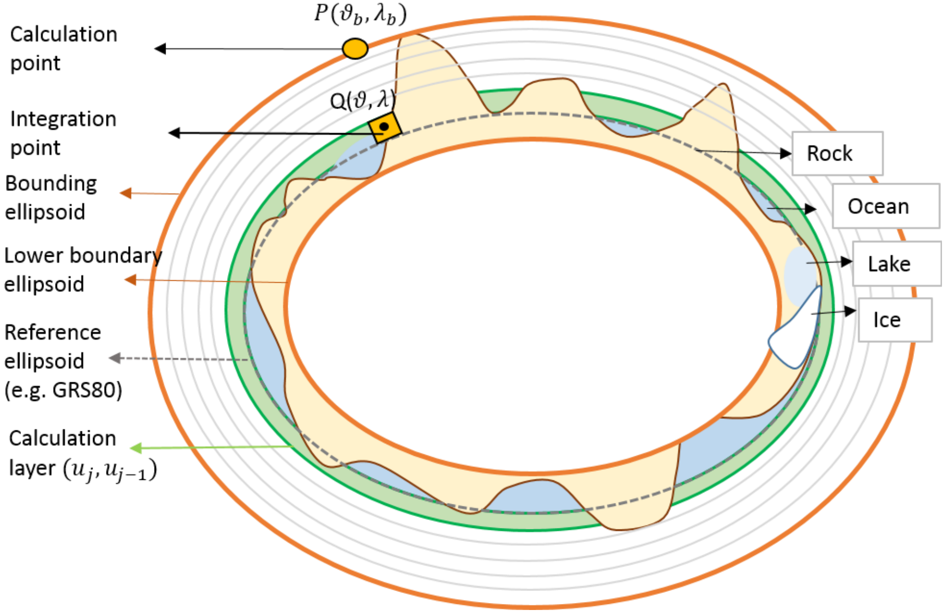

ROLI Topographic Gravity Field Model (2)

- Reciprocal distance between the calculation and integration points is expanded in terms of elementary ellipsoidal harmonics

$$\frac{1}{\ell} = \frac{1}{E}\sum_{n=0}^{\infty}\sum_{m=0}^{n}\frac{1}{2n+1} q_{nm}(\sigma_b) p_{nm}(\sigma) \times \left[\bar{R}_{nm}(\vartheta_b,\lambda_b)\bar{R}_{nm}(\vartheta,\lambda) + \bar{S}_{nm}(\vartheta_b,\lambda_b)\bar{S}_{nm}(\vartheta,\lambda)\right]$$

$$\left.\begin{matrix}\bar{R}_{nm}(\vartheta,\lambda)\\ \bar{S}_{nm}(\vartheta,\lambda)\end{matrix}\right\} = \bar{P}_{nm}(\cos\vartheta)\left\{\begin{matrix}\cos m\lambda\\ \sin m\lambda\end{matrix}\right. \qquad \sigma_b = \frac{b}{E}, \quad \sigma = \frac{u}{E}$$

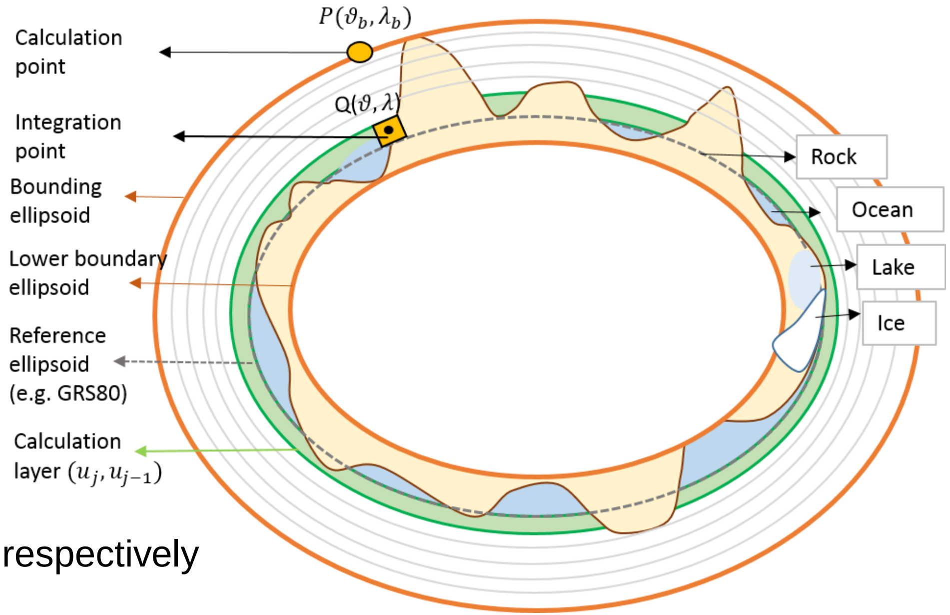

$q_{nm}(\sigma_b)$ and $p_{nm}(\sigma)$ are real functions proportional to Legendre functions of 2nd and 1st kind respectively

b semi minor axis of bounding ellipsoid, u semi minor axis of the ellipsoid of integration point, E linear eccentricity.

ROLI Topographic Gravity Field Model (3)

- The shells between two confocal ellipsoids are represented that are independent of the vertical density variation
- The gravitational potential of the topographic masses is expressed in terms of ellipsoidal harmonics

$$V = GE^3 \sum_{n=0}^{N} \sum_{m=0}^{n} \left[\bar{A}_{nm} \bar{R}_{nm}(\vartheta_b, \lambda_b) + \bar{B}_{nm} \bar{S}_{nm}(\vartheta_b, \lambda_b) \right]$$

where the coefficients are volume integrals

$$\bar{A}_{nm} = \frac{q_{nm}(\sigma_b)}{2n+1} \iiint \rho p_{nm}(\sigma) \bar{R}_{nm}(\vartheta, \lambda) \left(\sigma^2 + \cos^2 \vartheta \right) \sin \vartheta \, d\vartheta \, d\lambda \, d\sigma$$

$$\bar{B}_{nm} = \frac{q_{nm}(\sigma_b)}{2n+1} \iiint \rho p_{nm}(\sigma) \bar{S}_{nm}(\vartheta, \lambda) \left(\sigma^2 + \cos^2 \vartheta \right) \sin \vartheta \, d\vartheta \, d\lambda \, d\sigma$$

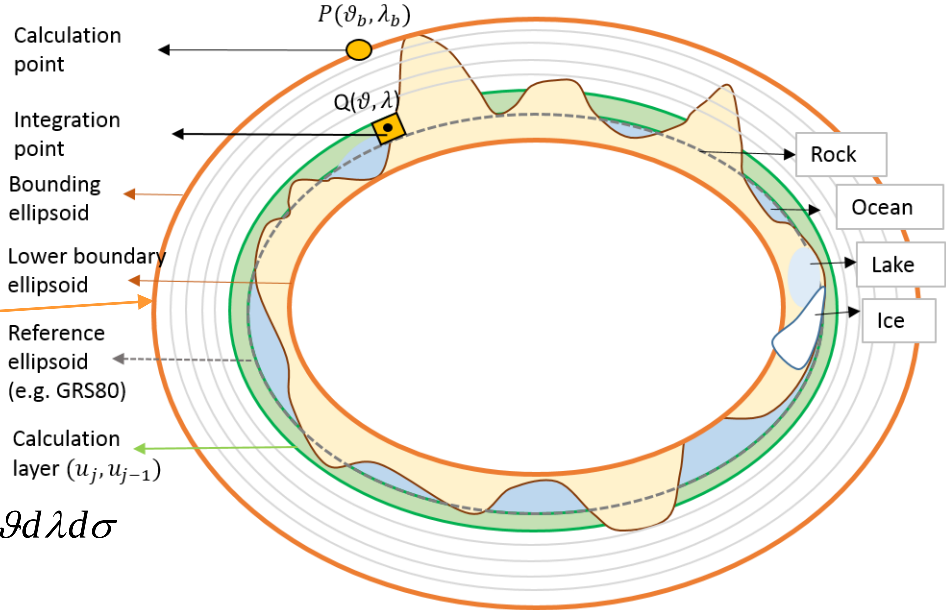

ROLI Topographic Gravity Field Model (4)

- The coefficients are represented as sums of potential coefficients corresponding to each shell:

$$\bar{A}_{nm} = \sum_j \bar{A}_{nm}^{j-1,j} \qquad \bar{B}_{nm} = \sum_j \bar{B}_{nm}^{j-1,j}$$

- Finally, we put all the coefficients above degree n=3600 to be equal to zero:

$$\left\{\bar{A}_{nm} = \bar{B}_{nm} = 0\right\}_{n>3600}$$

and apply Jekeli’s transformation to obtain spherical harmonic coefficients $\left\{\bar{C}_{nm}, \bar{S}_{nm}\right\}_{n\leq 3660}$ of ROLI_SphN_3660.

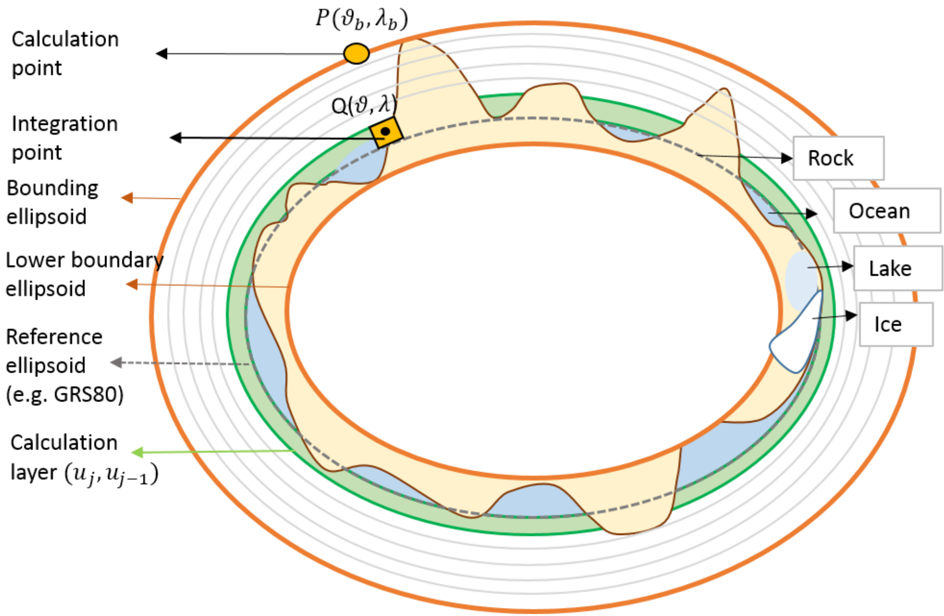

Input data - Earth 2014

- The latest Earth's relief model Earth2014 as input (Hirt and Rexer, 2015).
- 1′x 1′ global grids for five files are used as input this study
  - SUR (Earth's surface)
  - BED (Earth's bedrock)
  - TBI (Topography, bedrock and ice)
  - ICE (Major ice sheets) and
  - Landtypes mask (MSK2014_landtypes.1min.geod.bin)

Comparisons wrt other models of its kind

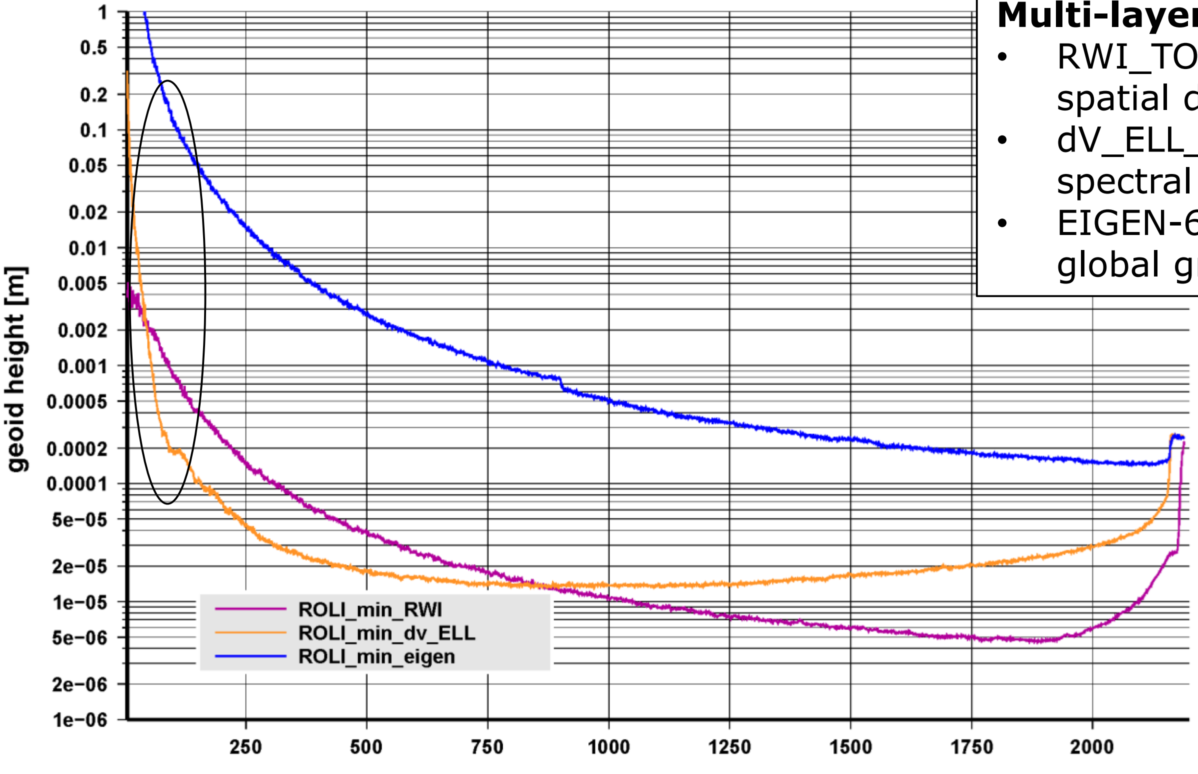

Degree amplitudes

Multi-layer approach (rock, ocean, lake, ice)
- RWI_TOPO_2015 (Grombein et al. 2016) in spatial domain
- dV_ELL_Earth2014 (Rexer et al. 2016) in spectral domain
- EIGEN-6C4 (Förste et al.,) representation global gravitational field of the Earth

The intention is to use the topographic gravity field model to represent the high degree order components of the gravity field.

HELMHOLTZ

ROLI_SphN_3660 (d/o 3660) vs RWI_TOPO_2015 (d/o 2190)

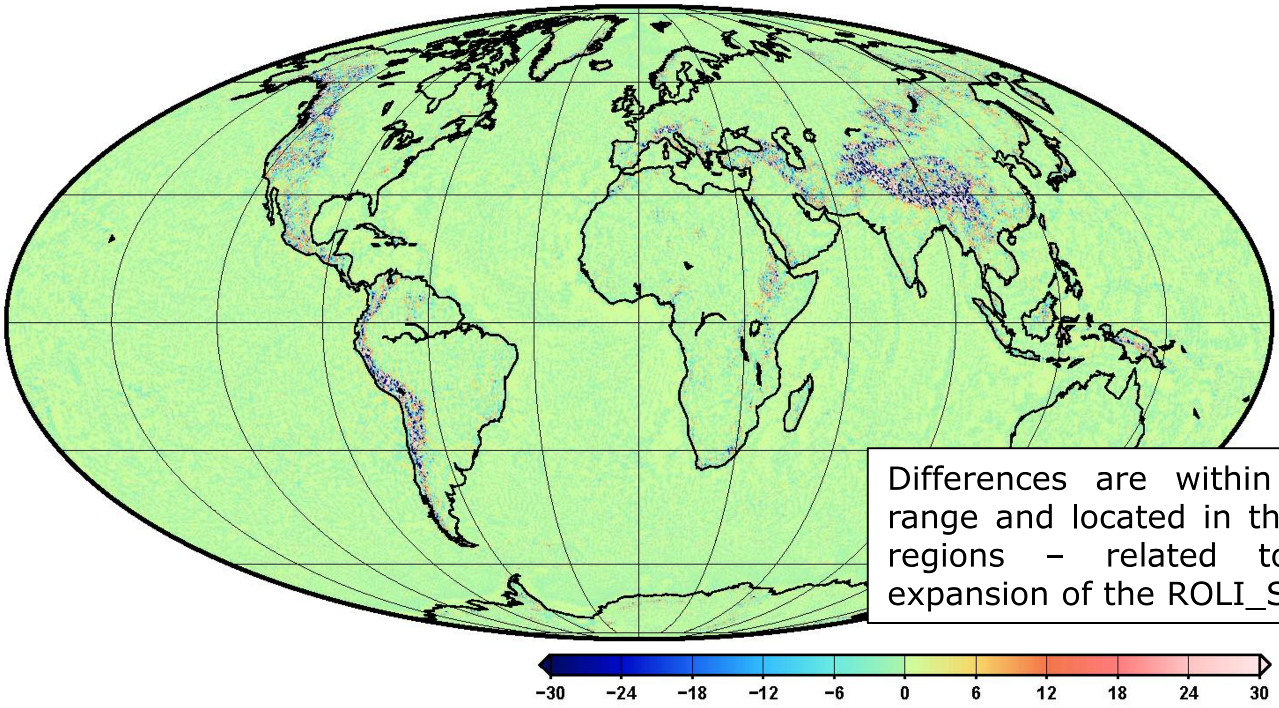

Differences are within the expected range and located in the mountainous regions – related to the higher expansion of the ROLI_SphN_3660

dg_ROLI_SphN_3660_plusGRS80_minus_dg_RWI_TOPO_2015_plusGRS80

δg_{SA}, 0.25° x 0.25°

wrms about mean / min / max = 7.981 / −324.1 / 417.1 mgal

GFZ Helmholtz Centre POTSDAM

HELMHOLTZ

ROLI_SphN_3660 (d/o 3660) vs dv_ELL_Earth2014 (d/o 2190) (1)

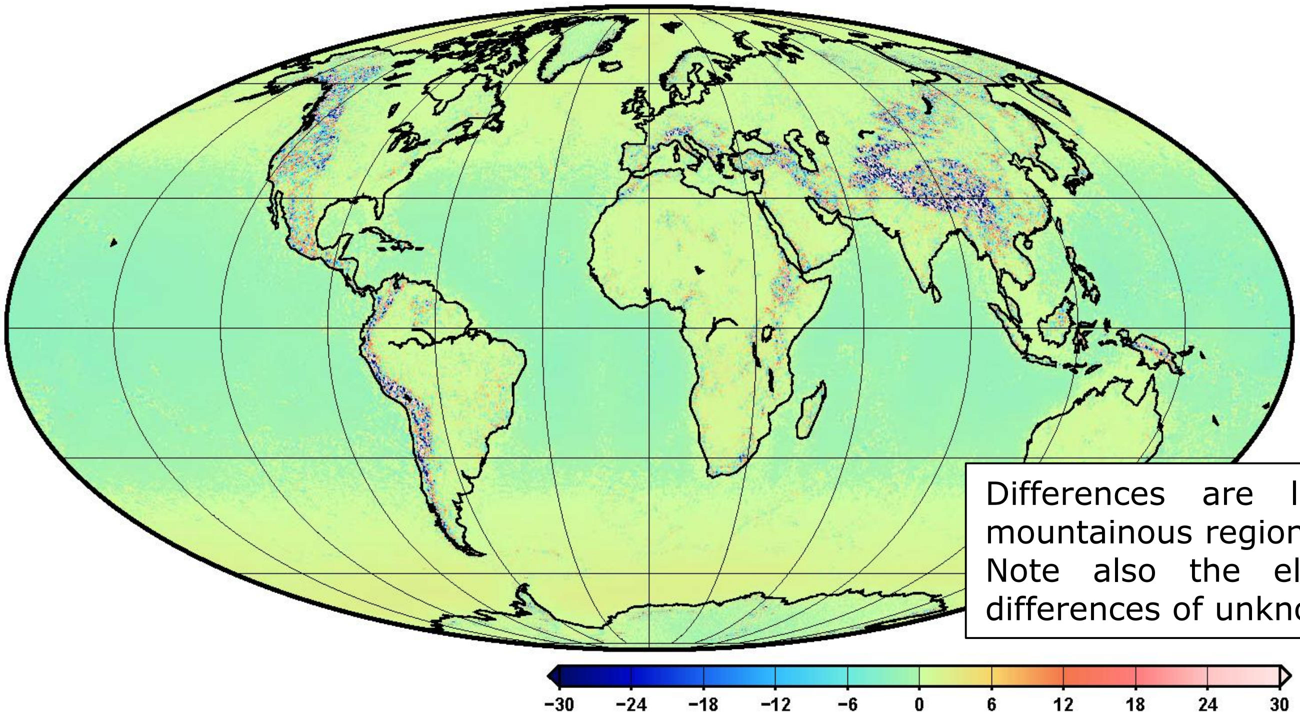

dg_ROLI_SphN_3660_plusGRS80_minus_dg_dV_ELL_Earth2014_plusGRS80
δg_{SA}, 0.25° x 0.25°
wrms about mean / min / max = 8.169 / −326.3 / 415.2 mgal

Differences are located in the mountainous regions.
Note also the ellipsoidal shape differences of unknown source.

ROLI_SphN_3660 (d/o 3660) vs dv_ELL_Earth2014 (d/o 2190) (2)

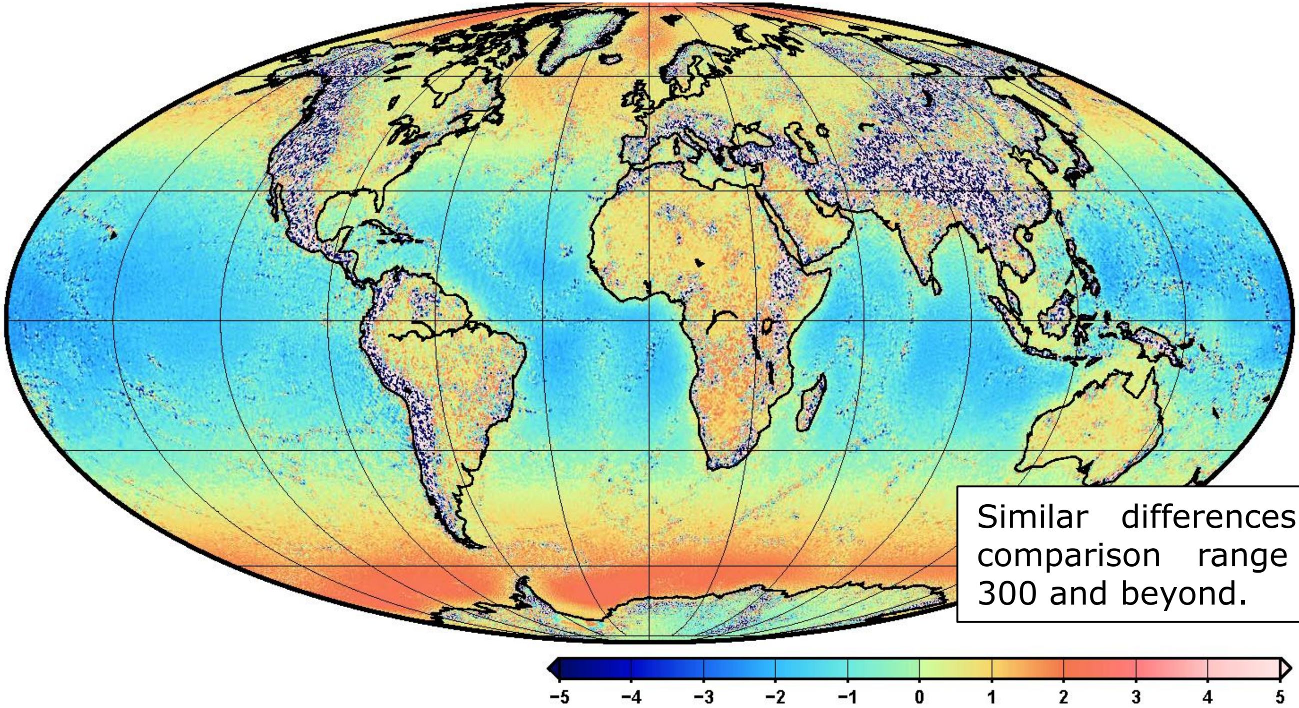

Similar differences exist in the comparison range between d/0 300 and beyond.

dg_ROLI_SphN_3660_plusGRS80_300.3660_minus_dg_dV_ELL_Earth2014_plusGRS80_300.2190
δg_{SA}, 0.25° x 0.25°
wrms about mean / min / max = 8.169 / −326.3 / 415.2 mgal

Blended model (EIGEN-6C4 + ROLI_SphN_3660)

↓

High resolution combined static gravity field models

(blending in the spherical harmonic coefficient level)

2 Blended Test Models

1- EIGEN-6C4.300.500.ROLI_SphN_3660

2- EIGEN-6C4.2000.2100.ROLI_SphN_3660

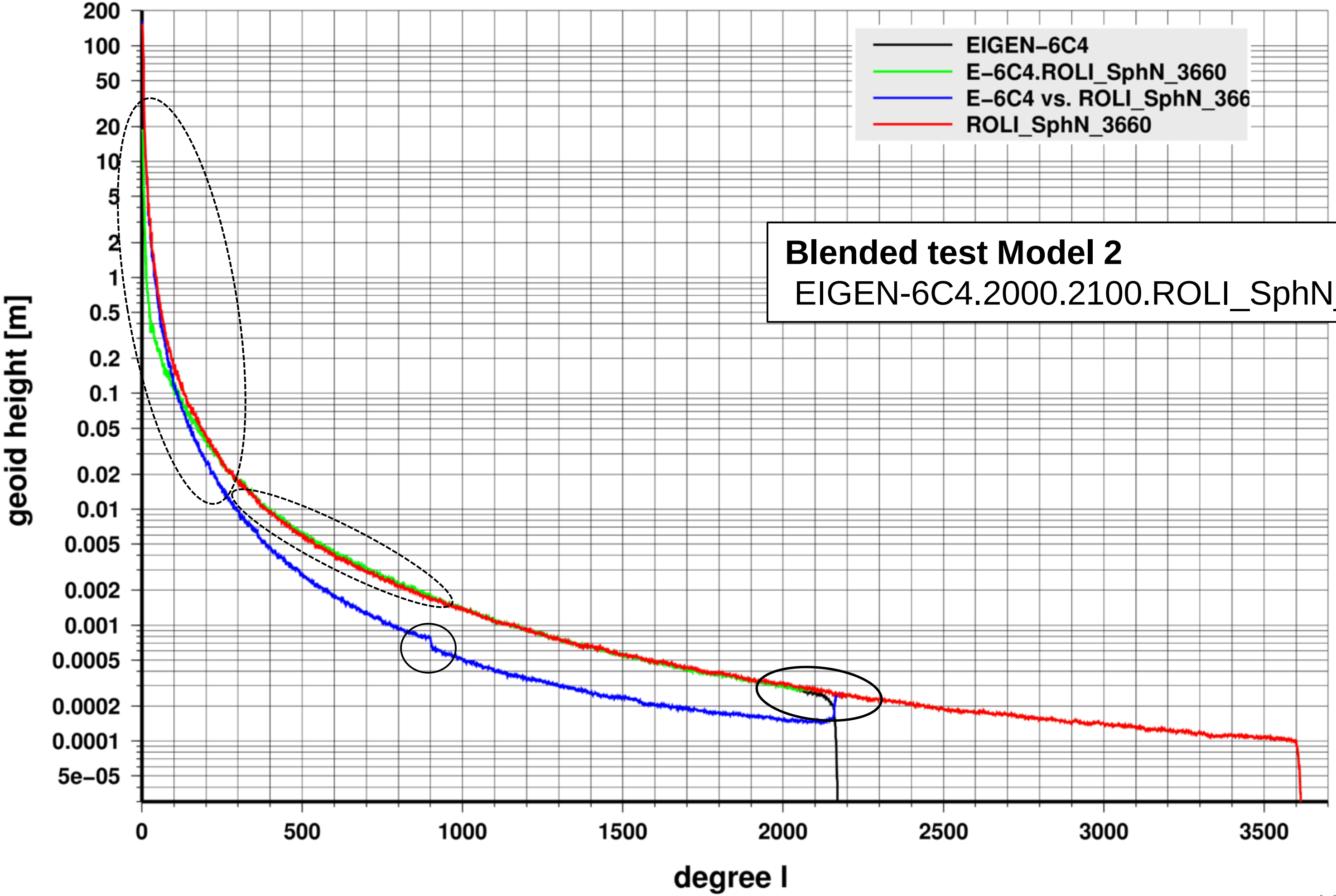

Blended test Model 2
EIGEN-6C4.2000.2100.ROLI_SphN_3660

Contribution of ROLI_SphN_3660 to EIGEN-6C4

The blended model is augmented using ROLI_SphN_3660 with a transition range between 2000 and 2100

Promising reduction of omission error in future generation EIGEN series

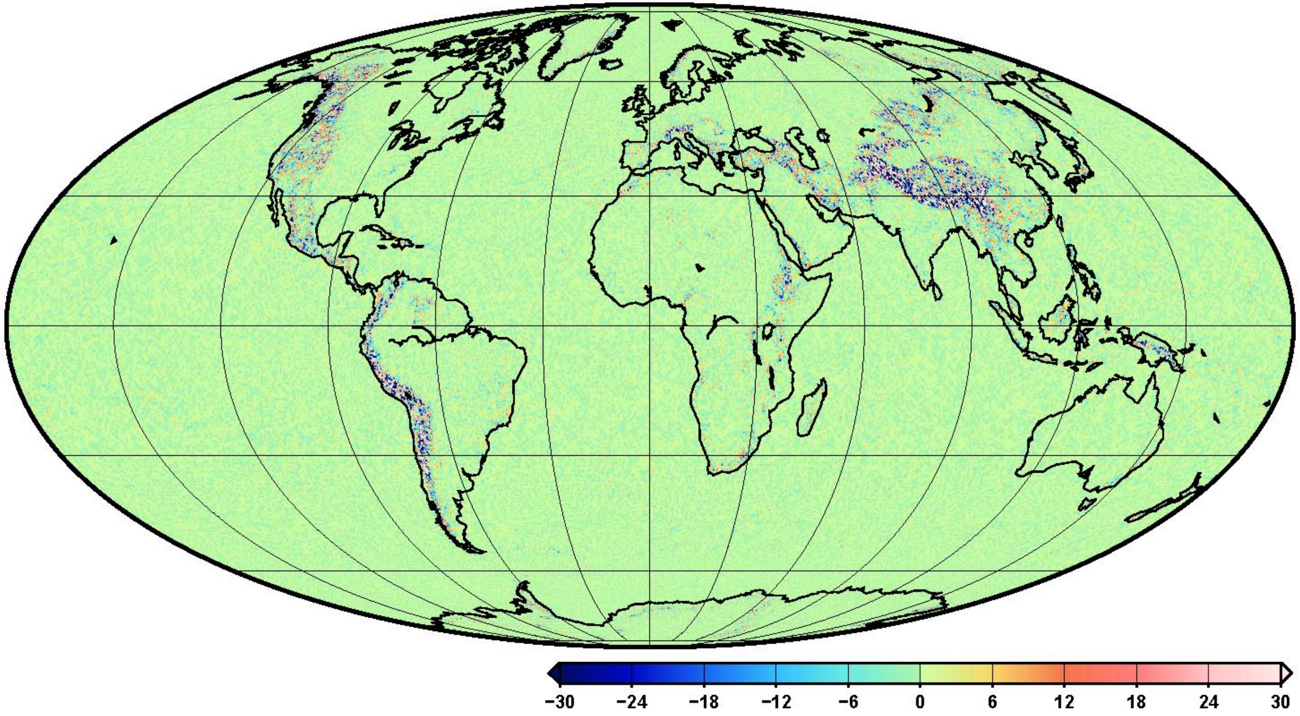

dg_diff_eigen6c4_2190_EIGEN−6C4v1.2000.2100.ROLI_3660
δg_{SA}, 0.25° x 0.25°
wrms about mean / min / max = 8.177 / −433.2 / 320.3 mgal

Blended model vs EIGEN- 6C4 only

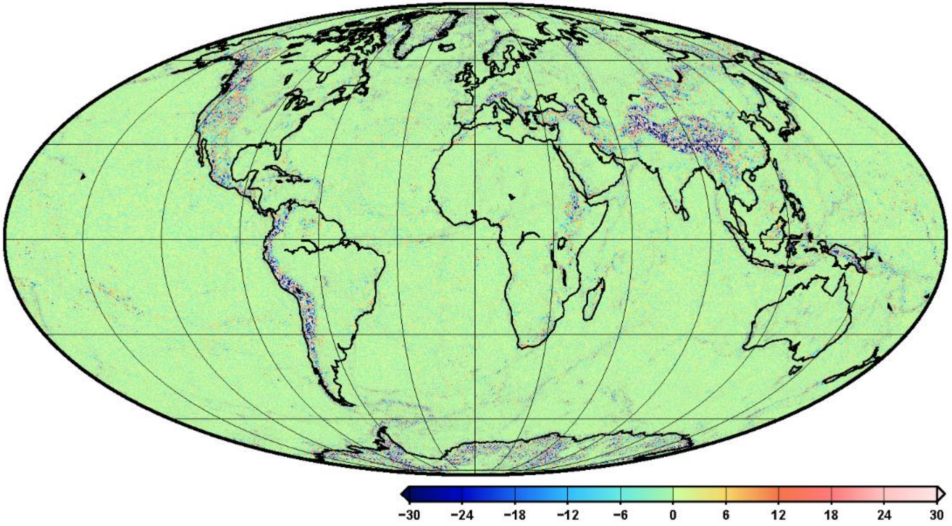

dg_eigen−6c4_minus_dg_EIGEN−6C4v1.300.500.ROLI_SphN_3660
δg_{SA}, 0.25° x 0.25°
wrms about mean / min / max = 10.87 / −482 / 412.4 mgal

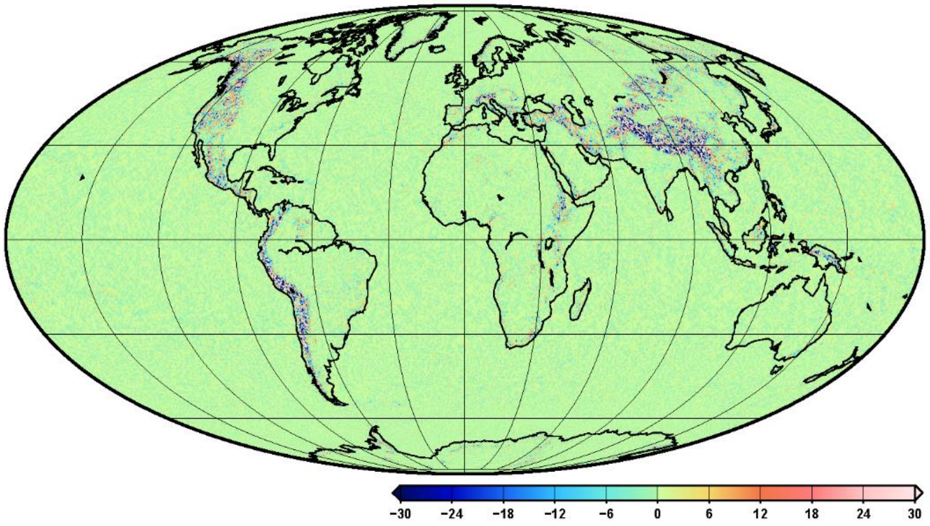

dg_eigen−6c4_minus_dg_EIGEN−6C4v1.2000.2100.ROLI_SphN_3660
δg_{SA}, 0.25° x 0.25°
wrms about mean / min / max = 8.177 / −433.2 / 320.3 mgal

Different regions will benefit from blending differently which needs to be investigated for the ideal global gravity field model.

GFZ
Helmholtz Centre
Potsdam

HELMHOLTZ

Blended vs EIGEN-6C4 only (filling the gappy regions)

Complementary to the regions with no or limited terrestrial gravity data.

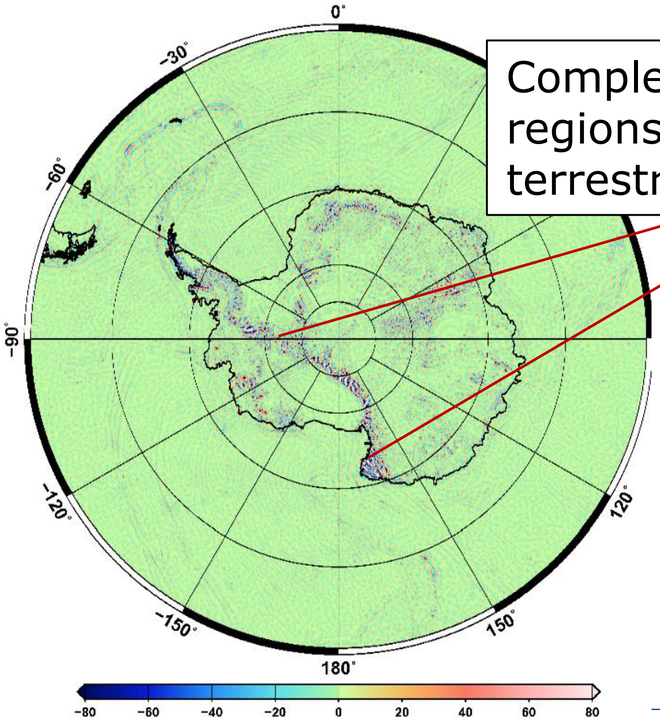

dg_eigen-6c4_SouthPole_minus_dg_EIGEN-6C4v1.300.500.ROI
δg_{SA}, 0.05° x 0.05°
wrms about mean / min / max = 10.63 / −411.1 / 230.2 mgal

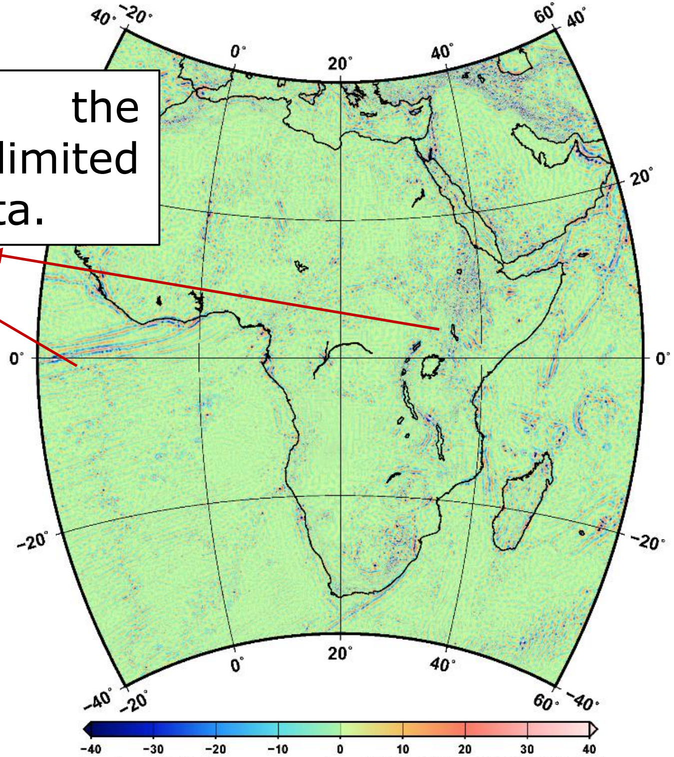

dg_eigen-6c4_Africa_minus_dg_EIGEN-6C4v1.300.500.ROLI_S
δg_{SA}, 0.05° x 0.05°
wrms about mean / min / max = 7.971 / −212.6 / 283.4 mgal

GFZ Helmholtz Centre Potsdam

Evaluation of blended model (1)

- Comparisons wrt GNSS/levelling derived geoid undulations in 7 different regions indicate only minor improvement in some of the regions
- This confirms that the improvement will not be in the long wavelength and in the regions where we have a good quality terrestrial gravity data coverage
- However, the same comparison should be done in regions where missing gravity measurements (not well covered areas)

Geoid/Height anomaly (cm)	max d/o	USA	Austr (HA)	Germ (HA)	Canada	Eur	Japan	Brazil
		6169	7841	470	1931	1047	816	672
EGM2008	2190	24,61	9,67	2,32	12,54	12,45	8,16	36,65
EIGEN-6C4	2190	24,50	9,08	2,22	12,39	12,05	7,75	30,65
EIGEN-6C4.2000.2100.ROLI_SphN_3660	3660	24,42	9,08	2,08	12,25	12,19	7,84	30,62

Sources/References for the used GPS/Lev data:
USA: (Milbert, 1998), **Canada:** (M. Véronneau, personal communication 2003, Natural Resources Canada), **Europe/Germany:** (Ihde et al., 2002), **Australia:** (W. Featherstone, Curtin University of Technology, personal communication 2018, c.f. W. Featherstone et al. 2018, https://doi.org/10.1080/08120099.2018.1412353), **Japan**: (Tokuro Kodama, Geospatial Information Authority of Japan, personal communication 2013), **Brazil**: Denizar Blitzkow and Ana Cristina Oliveira Cancoro de Matos, Centro de Estudos de Geodesia (CENEGEO), personal communication, the data belongs to the Brazilian Institute of Geography and Statistics (IBGE)

Evaluation of blended model (2)

dg: The comparison of gravity values shows significant improvement for the topographic model (reduction of RMS and Mean)

dN: Topographic model shows reduction in Mean but not necessarily rms values.

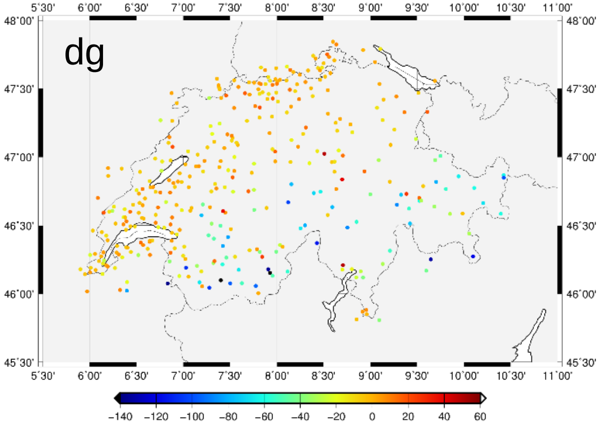

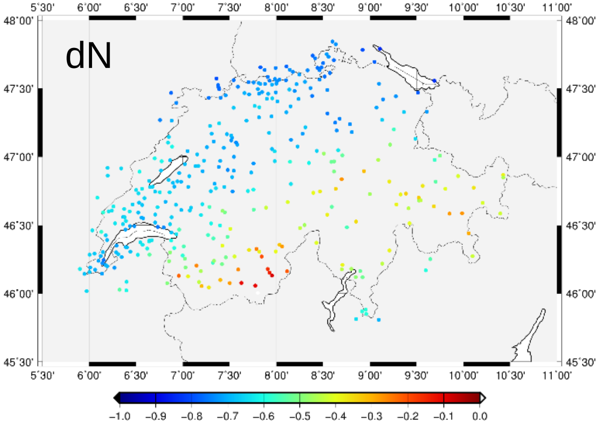

Marti U., 2015

swisstopo2004_geoid_a-358	max d/o	Gravity (on ground, mGal) / mean		Geoid (cm) / mean	
		rms [mGal]	mean [mGal]	rms [cm]	mean [cm]
egm2008	2190	39,694	-21,555	17,560	-63,592
EIGEN-6C4	2190	40,193	-21,224	14,261	-62,050
EIGEN-6C4.2000.2100.ROLI_SphN_3660	3660	**30,696**	**-14,757**	15,052	-60,084

Evaluation of blended model (4)

With the contribution of topographic gravity field model ROLI_SphN_3660, we see improvement for the two series along the NS and EW Germany.

The improvement is of about 10% which is significant for such data!

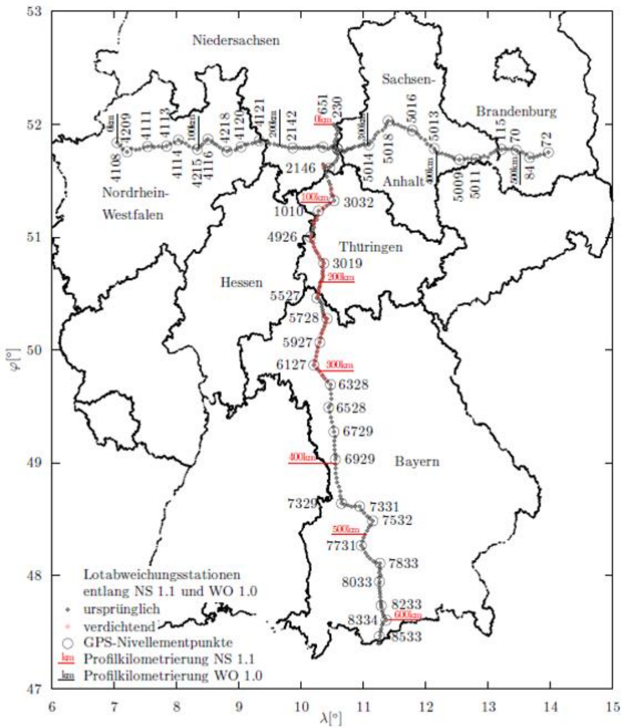

Abbildung 6.1. Astrogeodätische Lotabweichungsstationen und GPS-Nivellemer
Süd-Profils NS 1.1 und des ursprünglichen West-Ost-Profils WO 1.0

Voigt C., 2013

	Profile	ns2.0.red (216)		wo2.0.red (154)	
Deflection of the vertical (arcsec)		**Nord/South**	**East/West**	**Nord/South**	**East/West**
	max d/o	rms [arcsec]	rms [arcsec]	rms [arcsec]	rms [arcsec]
egm2008	2190	1,091	1,815	0,706	2,022
EIGEN-6C4	2190	1,094	1,805	0,706	2,022
EIGEN-6C4.2000.2100.ROLI_SphN_3660	**3660**	**0,917**	**1,614**	**0,511**	**1,951**

Conclusions

- A future EIGEN-x model could be generated from the latest LAGEOS, GRACE/GRACE-FO, GOCE data, the expected new DTU and Antarctic data and **our topographic model**
- Computation of Bouguer anomalies using gravitational potential and topographic potential
- Evaluation of gravitational potential using topographic potential and vice versa
- Local networks will benefit from the output of such models

ROLI_SphN_3660 vs dv_ELL_Earth2014_5480

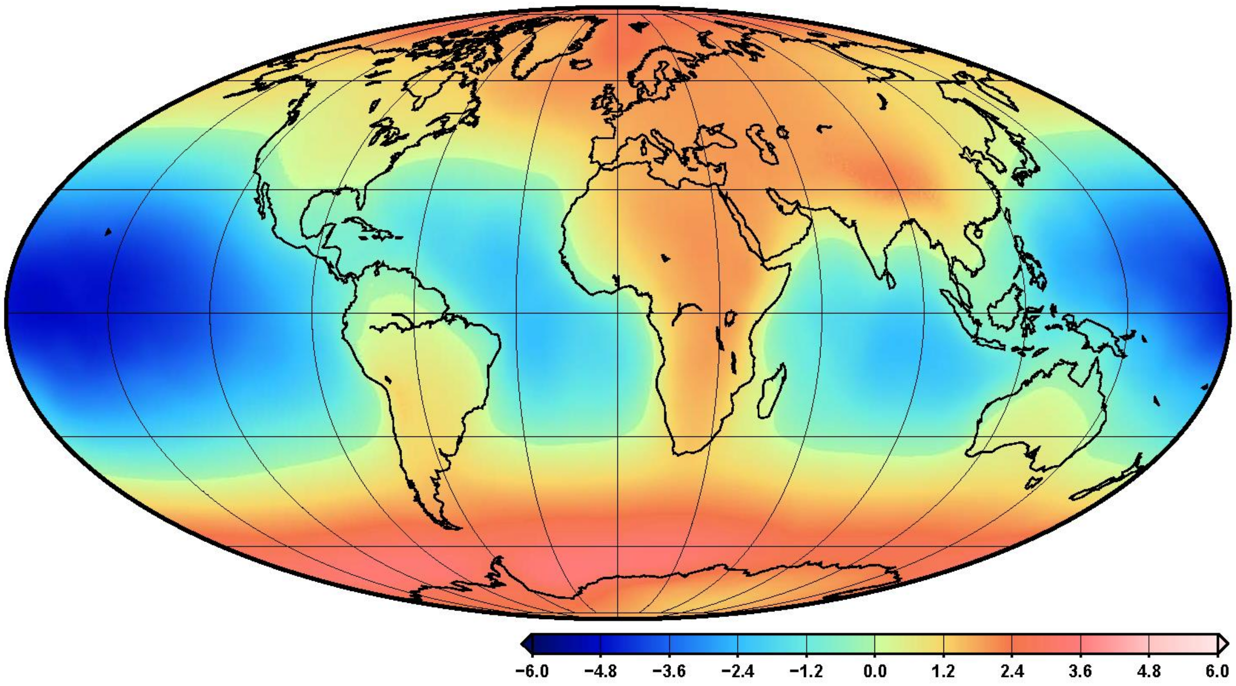

N_ROLI_SphN_3660_plusGRS80_minus_N_dV_ELL_Earth2014_plusGRS80
N, 0.25° x 0.25°
wrms about mean / min / max = 1.967 / −11.92 / −3.442 meter

GFZ Helmholtz Centre POTSDAM

HELMHOLTZ

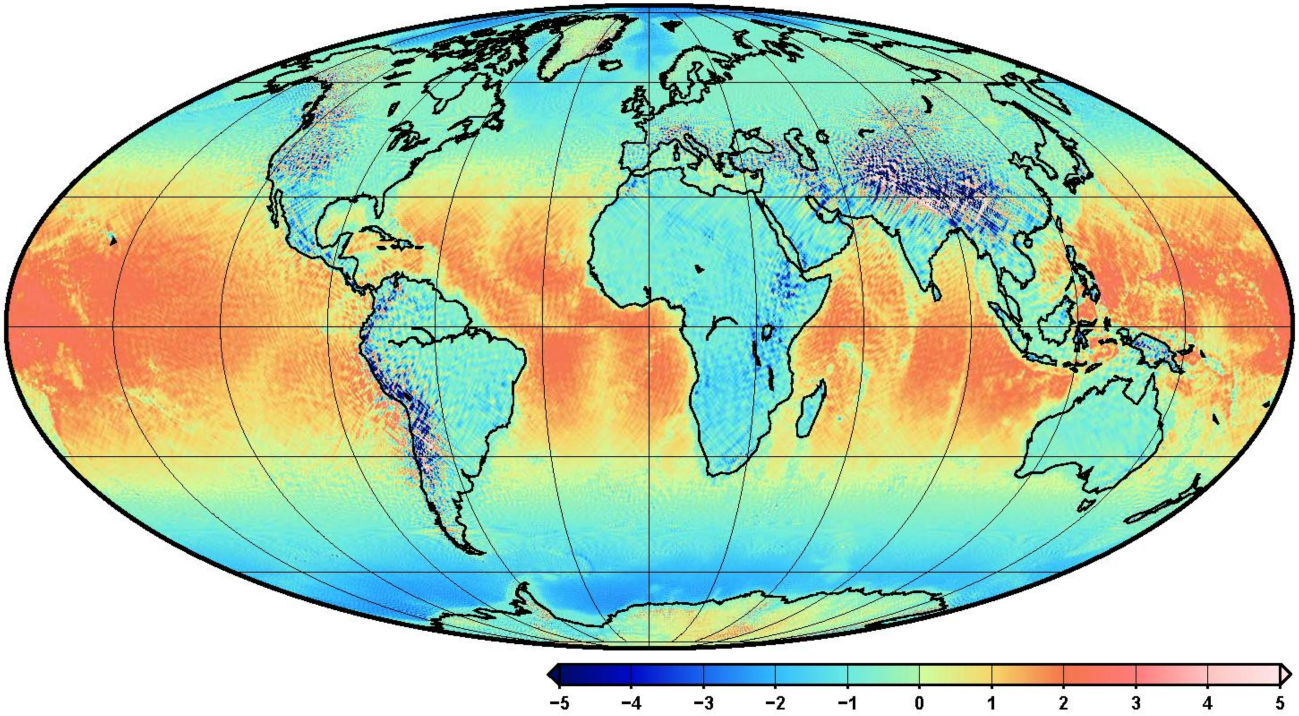

dg_dV_ELL_Earth2014_plusGRS80_300.2190_minus_dg_RWI_TOPO_2015_plusGRS80_300.2190
δg_{SA}, 0.25° x 0.25°
wrms about mean / min / max = 1.902 / −56.19 / 65.68 mgal

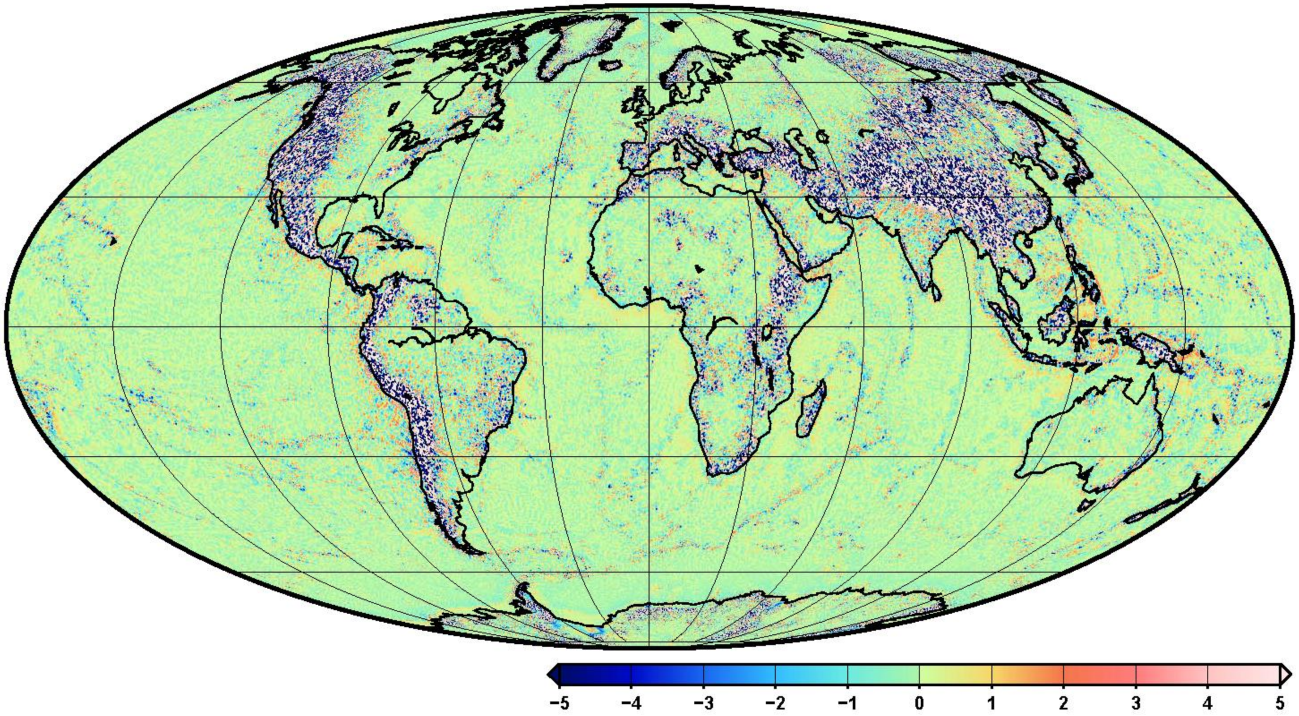

dg_ROLI_SphN_3660_plusGRS80_300.3660_minus_dg_RWI_TOPO_2015_plusGRS80_300.2190
δg_{SA}, 0.25° x 0.25°
wrms about mean / min / max = 7.981 / −324.1 / 417.1 mgal

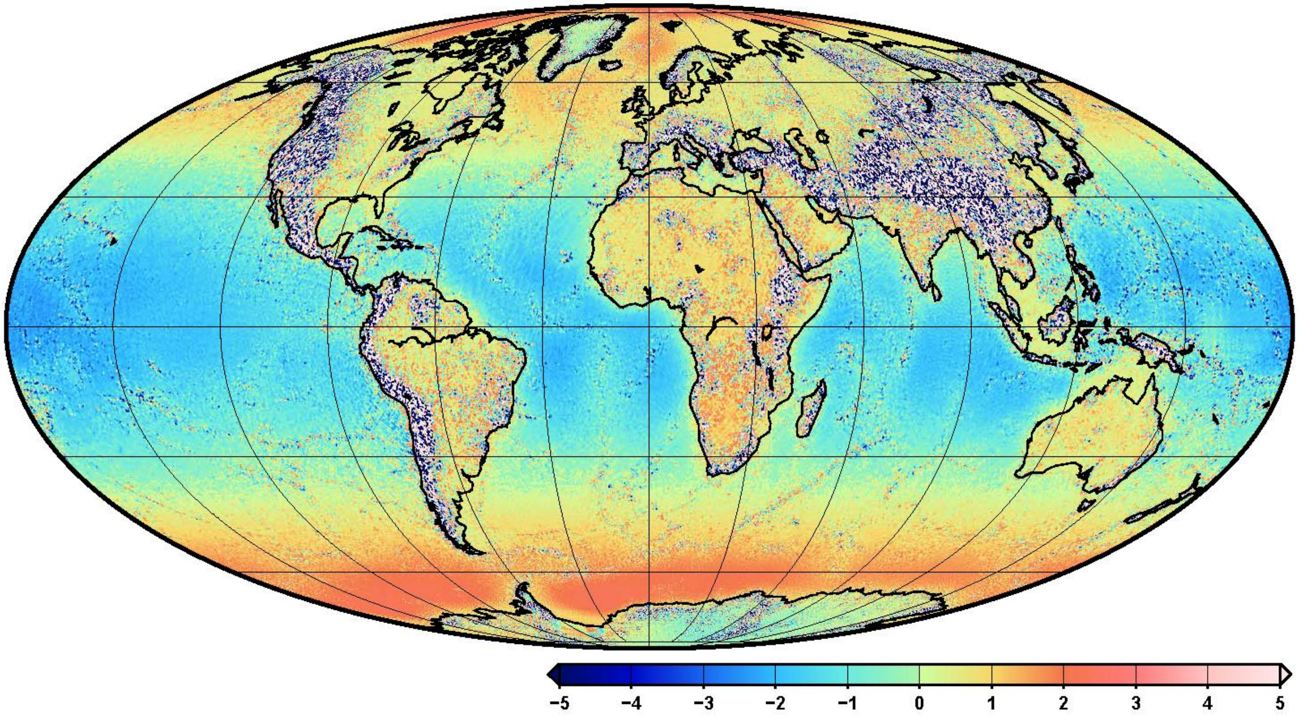

dg_ROLI_SphN_3660_plusGRS80_300.3660_minus_dg_dV_ELL_Earth2014_plusGRS80_300.2190
δg_{SA}, 0.25° x 0.25°
wrms about mean / min / max = 8.169 / −326.3 / 415.2 mgal

GFZ Helmholtz Centre POTSDAM

HELMHOLTZ

Evaluation of blended model (2)

Topographic model shows reduction of RMS for only one but decrease of Mean for all of the selected three data sets.

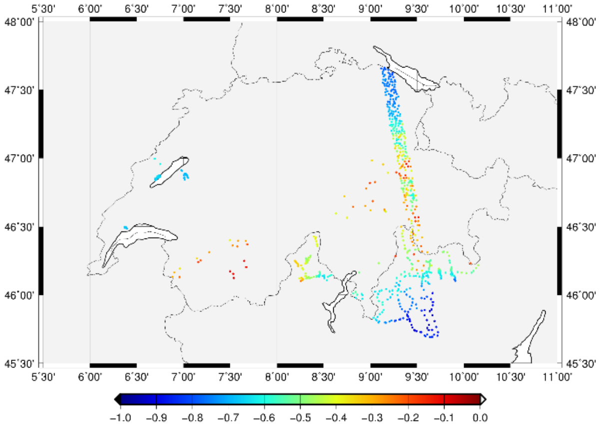

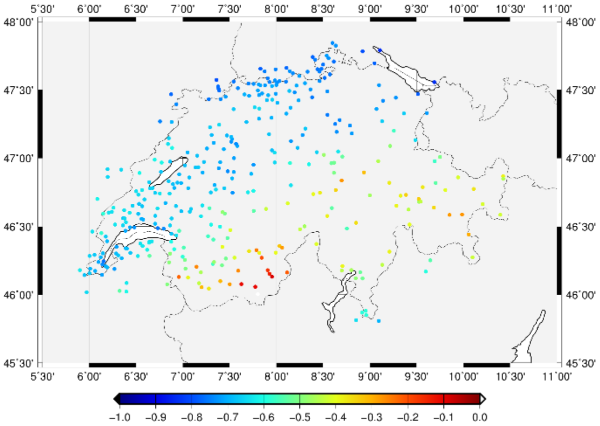

Geoid (cm) / mean	points	swisstopo2004_7000-geoid-648		swisstopo2004_geoid_a-358	
	max d/o	rms [cm]	mean [cm]	rms [cm]	mean [cm]
egm2008	2190	20,070	-55,884	17,560	-63,592
EIGEN-6C4	2190	18,804	-58,164	14,261	-62,050
EIGEN-6C4.2000.2100.ROLI_SphN_3660	3660	18,222	-56,406	15,052	-60,084

Evaluation of blended model (3)

The comparison of gravity values shows significant improvement for the topographic model (reduction of RMS and Mean)

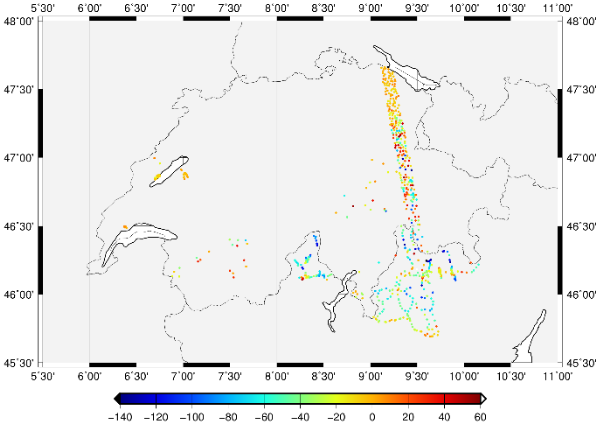

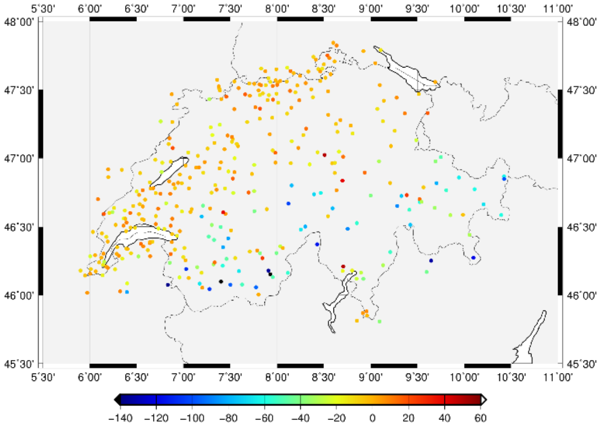

Gravity (on ground, mGal) / mean	points	swisstopo2004_ell-7000-648		swisstopo2004_ell-a-358	
	max d/o	rms [mGal]	mean [mGal]	rms [mGal]	mean [mGal]
egm2008	2190	47,650	-35,650	39,694	-21,555
EIGEN-6C4	2190	48,177	-36,137	40,193	-21,224
EIGEN-6C4.v1.2000.2100.ROLI_SphN_3660	3660	37,834	-25,161	30,696	-14,757

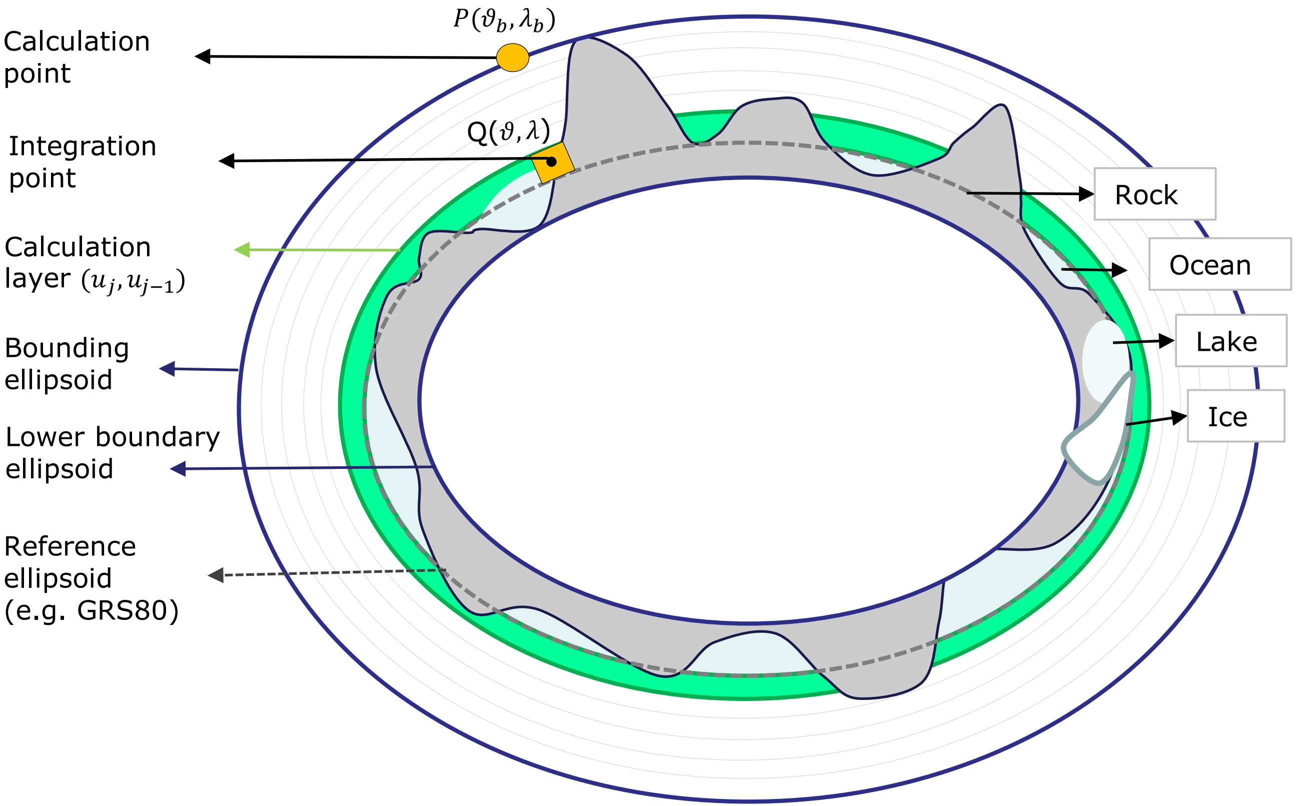

Calculation point
Integration point
Calculation layer (u_j, u_{j-1})
Bounding ellipsoid
Lower boundary ellipsoid
Reference ellipsoid (e.g. GRS80)
$P(\vartheta_b, \lambda_b)$
$Q(\vartheta, \lambda)$
Rock
Ocean
Lake
Ice

ROLI Topographic Gravity Field Model (3)

- The shells between two confocal ellipsoids are represented that are independent of the vertical density variation
- The gravitational potential of the topographic masses is expressed in terms of ellipsoidal harmonics

$$V = GE^3 \sum_{n=0}^{N} \sum_{m=0}^{n} \left[\bar{A}_{nm} \bar{R}_{nm}(\vartheta_b, \lambda_b) + \bar{B}_{nm} \bar{S}_{nm}(\vartheta_b, \lambda_b) \right]$$

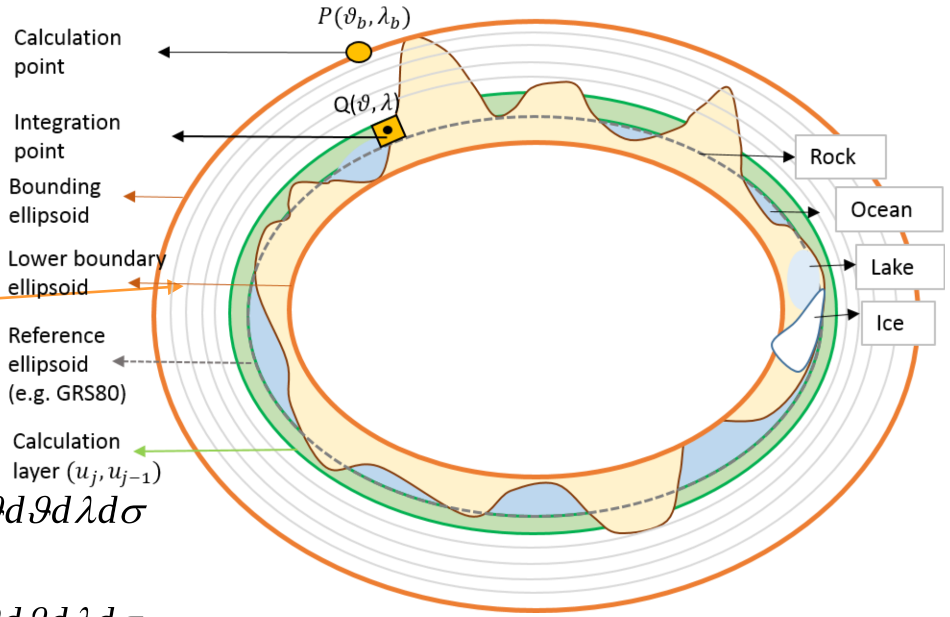

where the coefficients are volume integrals

$$\bar{A}_{nm} = \frac{q_{nm}(\sigma_b)}{2n+1} \iiint \rho p_{nm}(\sigma) \bar{R}_{nm}(\vartheta, \lambda) \left(\sigma^2 + \cos^2 \vartheta \right) \sin \vartheta \, d\vartheta \, d\lambda \, d\sigma$$

$$\bar{B}_{nm} = \frac{q_{nm}(\sigma_b)}{2n+1} \iiint \rho p_{nm}(\sigma) \bar{S}_{nm}(\vartheta, \lambda) \left(\sigma^2 + \cos^2 \vartheta \right) \sin \vartheta \, d\vartheta \, d\lambda \, d\sigma$$

ROLI Topographic Gravity Field Model (4)

- The coefficients are represented as sums of potential coefficients corresponding to each shell:

$$\bar{A}_{nm} = \sum_j \bar{A}_{nm}^{j-1,j} \qquad \bar{B}_{nm} = \sum_j \bar{B}_{nm}^{j-1,j}$$

$$\bar{A}_{nm}^{j-1,j} = \frac{q_{nm}(\sigma_b)}{2n+1} \left\{ \bar{\alpha}_{nm}^{j-1,j} \int_{\sigma_{j-1}}^{\sigma_j} \sigma^2 p_{nm}(\sigma) d\sigma + \left(F_{nm}^{-2} \bar{\alpha}_{n-2,m}^{j-1,j} + F_{nm}^{0} \bar{\alpha}_{nm}^{j-1,j} + F_{nm}^{+2} \bar{\alpha}_{n+2,m}^{j-1,j} \right) \int_{\sigma_{j-1}}^{\sigma_j} p_{nm}(\sigma) d\sigma \right\}$$

$$\bar{B}_{nm}^{j-1,j} = \frac{q_{nm}(\sigma_b)}{2n+1} \left\{ \bar{\beta}_{nm}^{j-1,j} \int_{\sigma_{j-1}}^{\sigma_j} \sigma^2 p_{nm}(\sigma) d\sigma + \left(F_{nm}^{-2} \bar{\beta}_{n-2,m}^{j-1,j} + F_{nm}^{0} \bar{\beta}_{nm}^{j-1,j} + F_{nm}^{+2} \bar{\beta}_{n+2,m}^{j-1,j} \right) \int_{\sigma_{j-1}}^{\sigma_j} p_{nm}(\sigma) d\sigma \right\}$$

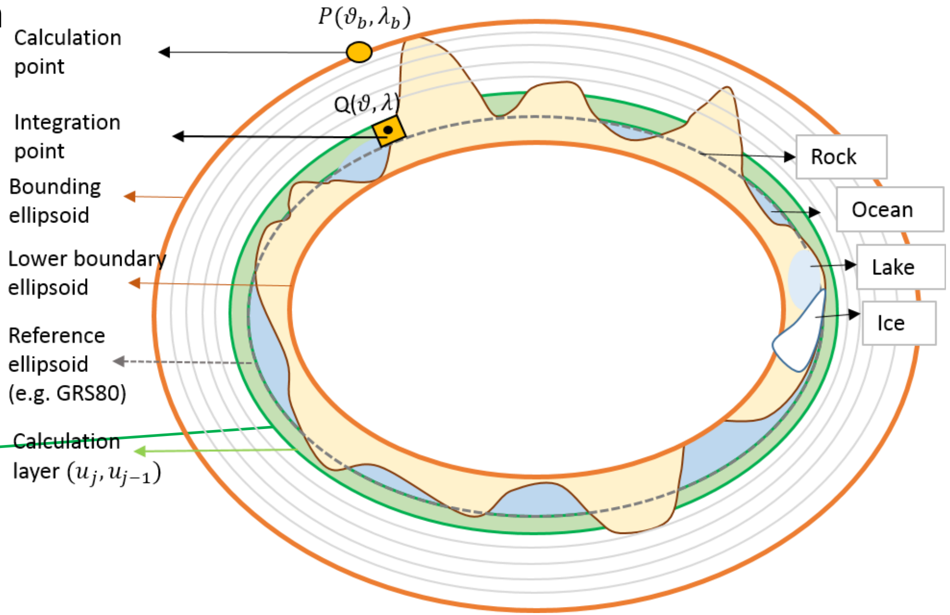

ROLI Topographic Gravity Field Model (5)

- On the previous slide $\bar{\alpha}_{nm}^{j-1,j}$, $\bar{\beta}_{nm}^{j-1,j}$ are coefficients of expansion of density in shell j into series of surface harmonics:

$$\rho_{j-1,j}(\vartheta,\lambda)=\sum_{n=0}^{N}\sum_{m=0}^{n}\left[\bar{\alpha}_{nm}^{j-1,j}\bar{R}_{nm}(\vartheta,\lambda)+\bar{\beta}_{nm}^{j-1,j}\bar{S}_{nm}(\vartheta,\lambda)\right]$$

and factors F_{nm}^{-2}, F_{nm}^{0}, F_{nm}^{+2} are:

$$\left.\begin{aligned}
F_{nm}^{-2}&=\sqrt{\frac{\left[(n-1)^2-m^2\right]\left[n^2-m^2\right]}{(2n-3)(2n-1)^2(2n+1)}}\\
F_{nm}^{0}&=\frac{2n(n+1)-2m^2-1}{(2n-1)(2n+3)}\\
F_{nm}^{+2}&=\sqrt{\frac{\left[(n+1)^2-m^2\right]\left[(n+2)^2-m^2\right]}{(2n+1)(2n+3)^2(2n+5)}}
\end{aligned}\right\}$$